

One-shot active learning for globally optimal battery electrolyte conductivity

Fuzhan Rahmanian^{1,2}, Monika Vogler^{1,2}, Christian Wölke³, Peng Yan³, Martin Winter^{3,4}, Isidora Cekic-Laskovic³, Helge S. Stein^{1,2,*}

¹Helmholtz Institute Ulm, Applied Electrochemistry, Helmholtzstr. 11, 89081 Ulm, Germany

²Karlsruhe Institute of Technology, Institute of Physical Chemistry, Fritz-Haber-Weg 2, 76131 Karlsruhe, Germany

³Helmholtz-Institute Münster (IEK-12), Forschungszentrum Jülich GmbH, Corrensstraße 46, 48149 Münster, Germany

⁴MEET Battery Research Center, University of Münster, Corrensstraße 46, 48149 Münster, Germany.

⁴Helmholtz-Institute Münster (IEK-12), Forschungszentrum Jülich GmbH, Corrensstraße 46, 48149 Münster, Germany

Address correspondence to: helge.stein@kit.edu

Abstract

Non-aqueous aprotic battery electrolytes, among other requirements, need to perform well over a wide range of temperatures in practical applications. Herein we present a one-shot active learning study to find all conductivity optima, confidence bounds, and relating trends in the temperature range from 30 °C to 60 °C. This optimization is enabled by a high-throughput formulation and characterization setup guided by one-shot active learning utilizing robust and heavily regularized polynomial regression. Whilst there is an initially good agreement for intermediate and low temperatures, there is a need for the active learning step to globally improve the model. Optimized electrolyte formulations likely correspond to the highest physically possible conductivities within this system when compared to literature data. A thorough error propagation analysis yields a fidelity assessment of conductivity measurements and electrolyte formulation.

Introduction

High-conductivity electrolytes in secondary batteries are of paramount importance for ensuring high performance and reliability of each battery cell chemistry¹. In specialty applications such as aerospace or stationary storage² in remote locations, bespoke electrolytes are however necessary. High or low temperatures make the electrolyte a limiting performance factor^{3,4} e.g. in electric vehicles which suffer from relatively narrow optimal temperature windows of 15 °C to 35 °C^{1,2}. Many studies^{2,3,5} have thus been conducted to evaluate lithium-ion battery (LIB) electrolytes at low temperatures in respect to their conductivity, however to date there, is no comprehensive study that identifies optimal formulations and conductivity trends thereof at any practically reasonable temperature.

We therefore present a one-shot active learning study to find the optimally conducting electrolyte formulation at temperatures ranging between -30 °C and 60 °C. Active learning uses machine learned “black-box” models to predict maxima and uncertainties to iteratively discover global maxima and

reduce the model uncertainty. Typically these models are trained in small (down to single sample) batches starting from scratch such that an acquisition function taking the model uncertainty into account is necessary^{6,7}. Through the availability of an already very broadly covering dataset of lithium hexafluorophosphate (LiPF₆) in ethylene carbonate (EC), ethyl methyl carbonate (EMC) and propylene carbonate (PC) totaling 80 electrolyte formulations at 10 temperatures as described by Flores et al.⁸ we chose to perform one-shot active learning in a fully exploitative⁷ mode. This approach has been shown to increase the so-called “enhancement factor” by Rohr et al.⁷ by up to a factor of 10 given the right model and initial training dataset choice. This enhancement factor determines the increase in probability of finding a good material or process. There are however other research modes⁷ not explored in this study since the focus is on the pure conductivity optimization of battery electrolytes. However, a recent study by Flores et al.⁸ focused on the “understanding driven” research mode. Their symbolic regression approach⁸ works well for high temperatures but fails for highly concentrated liquid electrolytes at low temperatures, indicating a change in the physicochemical behavior. This study is enabled through a comprehensive dataset that generated machine learned suggestions that were proven by the experimentalists. Organizationally, this study is the human-in-the-loop version of the fully autonomous active learning study presented by Rahmanian et al.⁹.

Methods

An initial dataset of 80 electrolyte formulations was considered using an automated formulation and characterization setup¹⁰. Each electrolyte formulation contains EC, propylene carbonate PC, e EMC in a solvent/co-solvent mixture and LiPF₆ as the conducting salt. Formulations were characterized between -30 °C and 60 °C, at increments of 10 °C as described by Krishnamoorthy et al¹⁰. Performed conductivity measurements were repeated 5 to 7 times. Uncertainties for the experimental values are expressed by the min/max spread of the measured values. For each datapoint, the electrolyte formulation, conductivity and measurement temperature were recorded. Across all formulations the ratio of $(EC + PC) : EMC$ was fixed either at 3:7 or 1:1 by weight and the concentration of LiPF₆ was selected between 0.2 and 2.1 mol/kg. For model training and one-shot active learning, the mass ratios of PC and LiPF₆ were normalized and referenced as $r_{PC} = \frac{PC}{(PC + EC)}$ and $r_{LiPF_6} = \frac{LiPF_6}{(PC + EC)}$. The $(EC + PC) : EMC$ ratio was not considered during model training.

Model training and one-shot active learning

The dataset size poses the challenge of finding well performing models that are simple and interpretable¹¹. We therefore settle on polynomial regression¹² for our purely exploitative active learning study. Contrary to Flores et al.⁸ we do not consider inter temperature trends in model training. The basic setup is a strongly regularized polynomial regressor aiming to avoid multicollinearity^{13,14}, which is measured by variance inflation factors^{15–18}. The polynomial regressor¹², ridge regularization¹⁹, and hyperparameter tuning are performed using the scikit-learn library^{20–22}. From the fitted polynomial model a fine subsampling is performed across 10⁴ formulation ratios at a fixed grid spacing of 1 ratio-%. From this fine subsampling, the top one percentile for each temperature was reported to the experimentalists

resulting in a total of 100 formulation suggestions. A subset of 24 formulations was chosen by the experimentalists covering all suggestions for -30°C , 20°C and 60°C . Subsequent to the formulation and conductivity measurements of the new formulations, the model was retrained on the entire dataset. For hyperparameter tuning (details see S5) we performed a Bayesian search^{20,23} with a threefold cross validation. The best parameters are then fed to the surrogate model. This search uses ridge regularized polynomial models to favor low polynomial degrees. To assess the model uncertainty for both aleatoric and epistemic uncertainty after the learning shot (and the possible necessity for a second learning shot) we build a pipeline applying the model agnostic prediction interval estimator (MAPIE)²⁴. This estimator uses jackknife plus²⁵ to estimate the uncertainty²⁶ of the model for a 95% prediction interval. A summary of this study's workflow can be seen in Figure 1. Summarizing there are three stages in this pipeline: 1) model training, 2) formulation suggestion and measurement, 3) retraining and refinement of the model and uncertainty quantification.

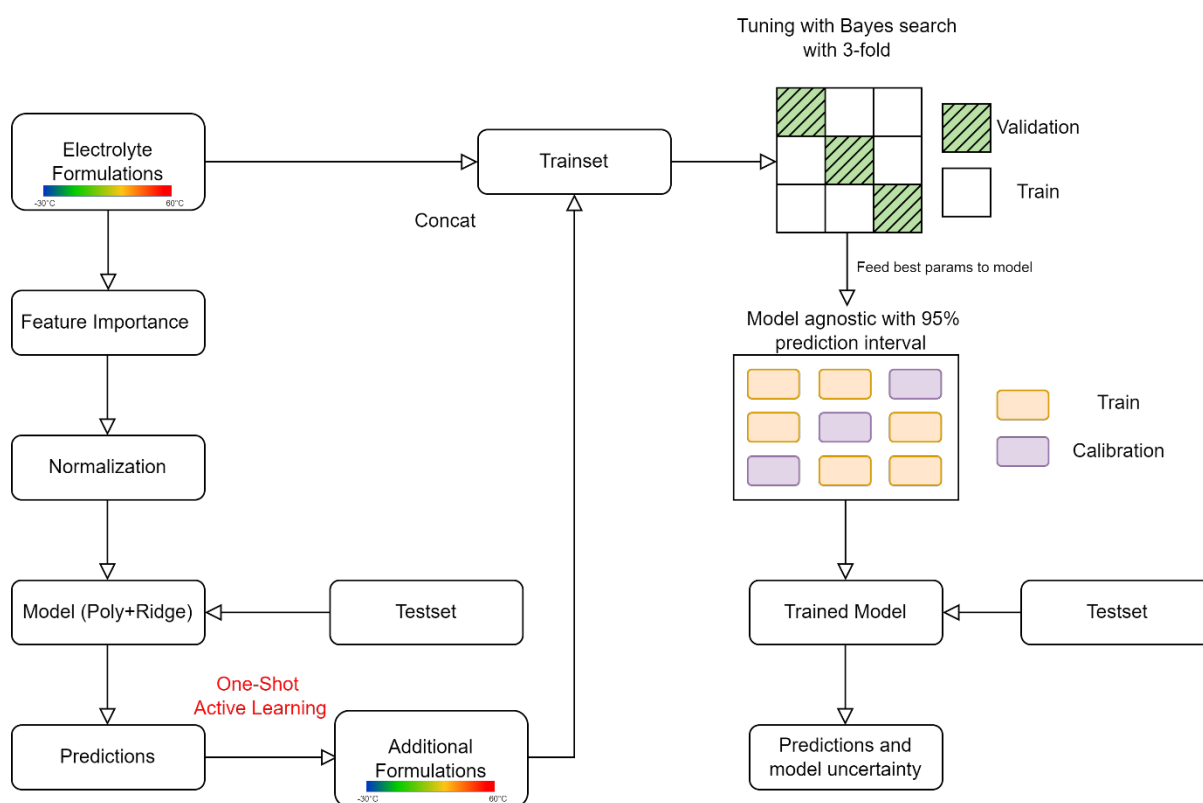


Figure 1: Schematic diagram of this study's pipeline consisting of initial model training, suggesting formulation to experimentalists for measurement of requested formulations and retraining the model by one-shot active learning with uncertainty quantification

Results and Discussion

Pre-shot model training

This study uses the same dataset underlying the study presented by Flores et al.⁸ using the formulation and characterization setup reported by Krishnamoorthy et al.¹⁰. The herein presented one shot active learning approach is model free, meaning that we do not utilize any physics or chemistry knowledge except correct pose of the input (formulation) and output (conductivity) and a compartmentalization of the problem by temperature.

The global trends of electrolyte conductivity, captured by our model, are shown in Figure 2, which illustrates the conductivity (σ) over r_{LiPF_6} and r_{PC} at -30°C , -10°C , 30°C , and 50°C (additional temperatures see S2). For all considered temperatures the R^2 score is $\approx 0.73 - 0.80$, which indicates a good fit. However, the degree of the polynomial used for the fit is higher for the high temperatures compared to low temperatures. The orange datapoints indicate the train set formulations. Overall conductivity is strongly correlated with temperature as expected from Debye-Hückel-Onsager (DHO) theory^{27,28}. Consequently, we observe low conductivity for $r_{LiPF_6} > 0.8$ or < 0.1 . In general, we observe the maximum conductivity shifting towards higher conducting salt concentrations at higher temperatures as it was studied by Landesfeind et al.^{30,27,28}. The lowest overall measured conductivity is 1.94 mScm^{-1} at 30°C showing a generally less pronounced dependence on r_{PC} than on r_{LiPF_6} . This observation correlates with the concentration-conductivity relationship that is primarily dependent on conducting salt concentration³⁰.

Going from low to high temperatures, the system seems to allow for higher r_{PC} and r_{LiPF_6} ^{31,32} while yielding a high conductivity which is in good agreement with established theory. The model also seems to prefer little presence of PC at low temperatures for higher conductivity. Our finding is in line with Ding et al.³³ who reported that from low to high temperatures, electrolyte formulation first enriches in EC³⁴ then in PC which results in higher dielectric constant and consequently higher conductivity^{30,35}. A narrow global optimum at high temperatures at relatively high r_{PC} of ≈ 0.3 , however lower conducting salt concentrations at 30°C and 50°C can be observed. All but the -10°C optima exist near unsampled formulations. Based on the prediction of the trained model, 10 samples with highest predicted conductivity for each temperature were selected and reported to the experimentalists. The requested and considered formulations can be found in the https://github.com/BIG-MAP/electrolyte_optimization_one_shot_active_learning.

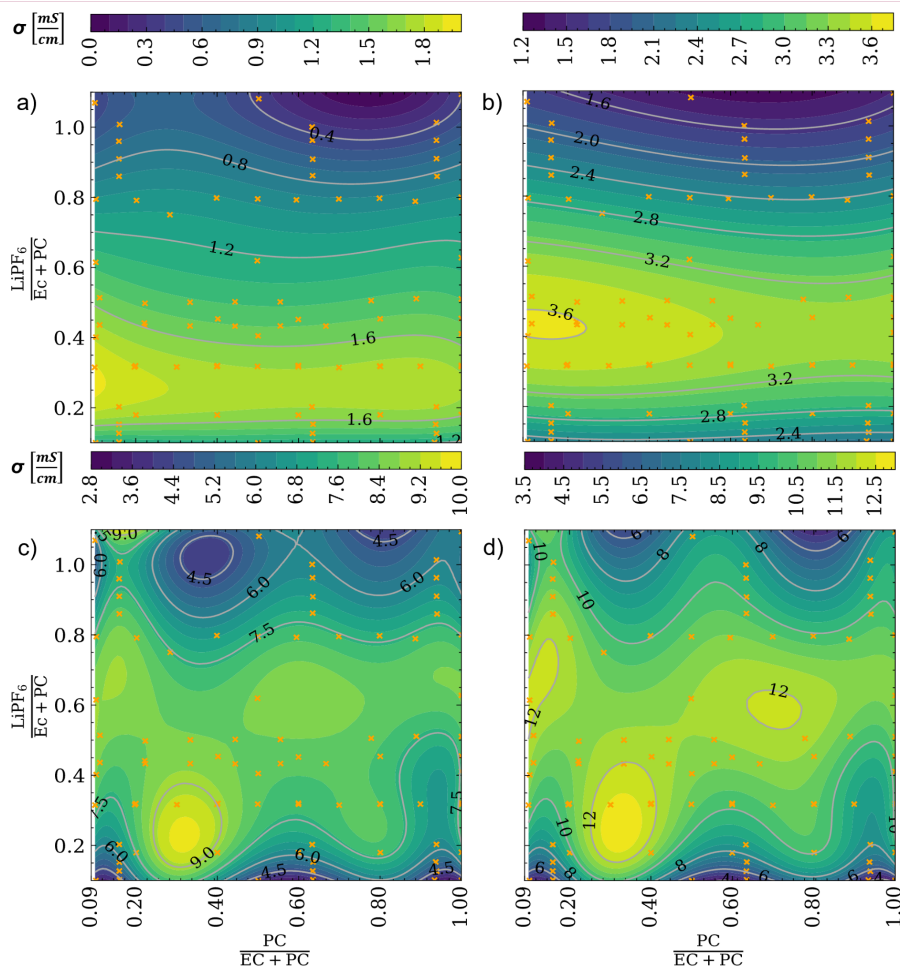


Figure 2: Trends in electrolyte conductivity at a) -30°C , b) -10°C , c) 30°C , d) 50°C . Orange data points represent the experimentally measured conductivity (σ) at the respective r_{PC} and r_{LiPF_6} . There is an overall incremental trend for higher r_{LiPF_6} from -30°C to -10°C and a narrow optimum in electrolyte conductivity at higher r_{PC} and lower r_{LiPF_6} at an unsampled formulation for high temperatures.

One-shot predictions and measurements

Utilizing the above polynomial models' results, shown in Figure 2, a total of 100 electrolyte formulation (1 percentile) in an intentionally full exploitation mode were selected and suggested to the experimentalists by only communicating the formulation and the respective temperature, however not the predicted conductivity. The experimentalists randomly selected 24 temperature optima from the suggested ones. These selected formulations correspond to temperatures of -30°C , 20°C and 60°C . Figure 3 compares the predicted and experimentally measured conductivity for the 24 selected formulations. There is a small deviation between the requested and actually measured formulations due to slight imperfections in the formulation process hence Figure 3 shows the conductivity prediction at the actually formulated composition. Inaccuracies occurring during the solid and liquid dispensing processes are technical in nature and are negligible given the fidelity assessment below. The error bar illustrates the conductivity error by reporting the maximum and minimum values among the repeated measurements.

The measured conductivities for the requested formulations are added as prior knowledge and the model is retrained. The regularization coefficient and polynomial degree are tuned subsequently using a Bayesian search optimization (See S5) and model uncertainty was incorporated using jackknife plus strategy (See S4).

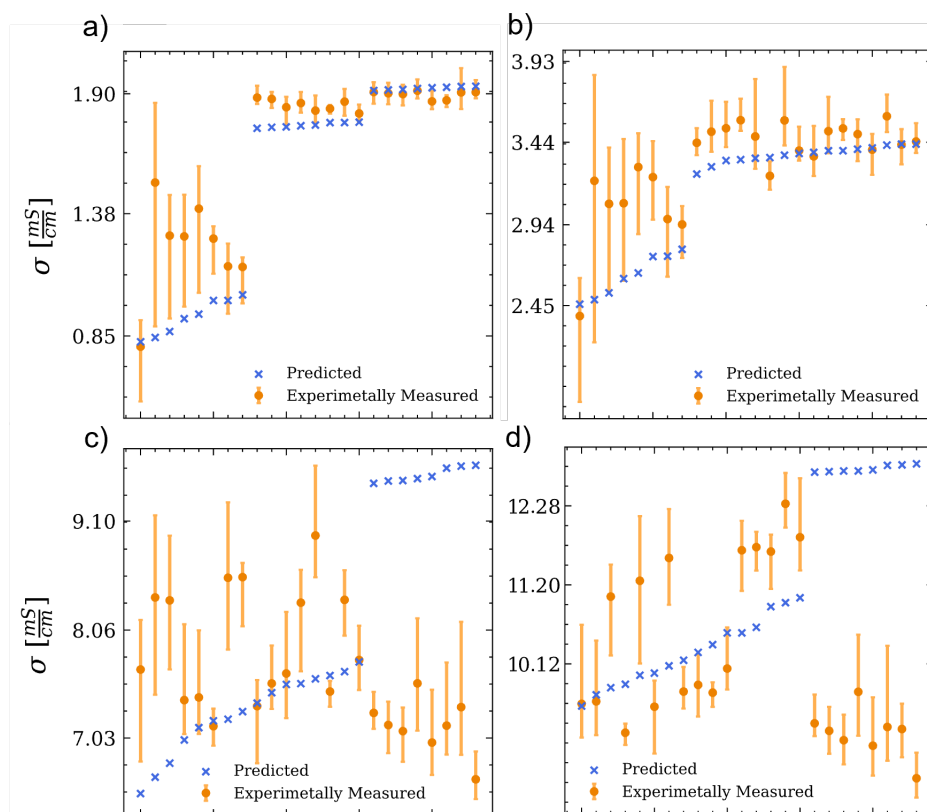


Figure 3: Comparison between measured and predicted conductivity values at a) -30°C , b) -10°C , c) 30°C , d) 50°C sorted by the predicted value at the respective temperature. Orange points represent the mean values of measured conductivities with error bars relating to the min/max from repeated measurements. The high accuracy for low temperature predictions is best observed in the sorted predictions in a) where the lowest 8 predictions were the formulations predicted to be best at 60°C , the intermediate 8 predictions were the optima for 20°C and the top 8 are the actual -30°C optima. Overall this suggests that there exists no globally optimal electrolyte and performance can vary by up to a factor of 2. Predictions for high temperatures are inaccurate suggesting a poor fit model.

Post-shot model refinement

After one-shot active learning and the Bayesian hyperparameter tuning (described in the methods section), models are significantly improved. The predicted trends for low temperatures changed only marginally whereas the improvements for temperatures of 30°C and 50°C are significant as shown in Figure 4 (additional temperatures in S3). Together with the low temperature trends there is now a coherent trend observed suggesting higher r_{PC} and r_{LiPF_6} at higher temperatures for the temperature refined optimal conductivity^{29,33}. This highlights the significance of active learning in model refinement as we only added an additional 30% of data points to the dataset whilst qualitatively improving the model. Comparing these results to the symbolic regression model by Flores et al⁸. reveals significant differences in the mass ratios required for maximum conductivity.

The drastic improvement of the model becomes even more obvious upon plotting the temperature maxima with the spread of the top percentile as displayed in Figure 5. Before the learning shot, the optima followed no physically meaningful or interpretable trend whereas after adding the extra data the very fine trends in optima towards higher r_{LiPF_6} and slightly more r_{PC} become obvious. Uncertainty quantification was performed using the jackknife plus strategy resulting in an average 95 % prediction uncertainty interval of $3 \cdot 10^{-3}$ mS/cm (See S4). However, the incorporation of the model agnostic prediction technique allows the measurement of aleatoric and epistemic uncertainty at any point. Comparing the results for electrolyte conductivity found by our one-shot active learning approach to literature such as Ding et al.²⁸ at 60 °C, and -30 °C suggests that the herein reported maxima corresponds to the global physical maximum conductivity in this system which is ≈ 12 mS/cm and 1.9 mS/cm. In another study, Landesfeind et. al.²⁹ indicate global maxima of 4.7 mS/cm, 7.6 mS/cm and 9.25 mS/cm at -10 °C, 20 °C, and 30 °C, respectively. Their results are compatible with our findings.

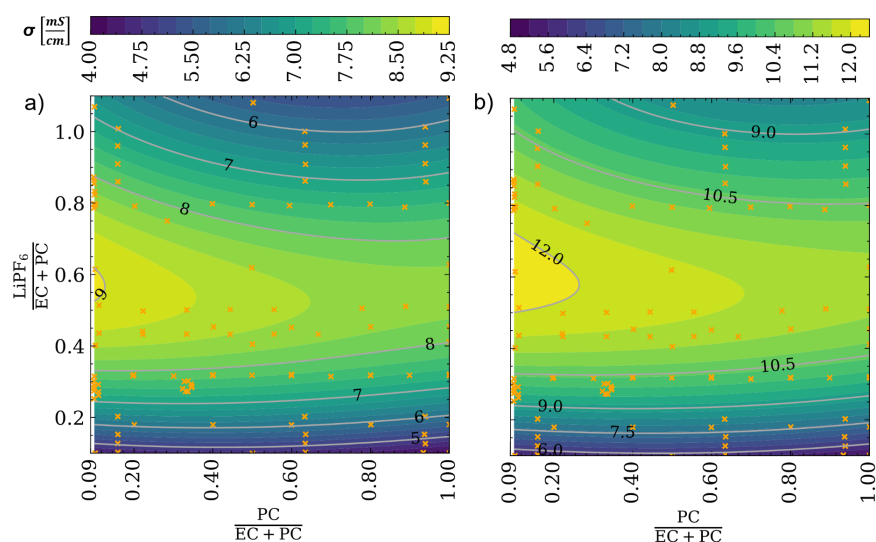


Figure 4: Trends in electrolyte conductivity after one shot active learning for optimizing the regressor at higher temperatures and understanding the underlying physicochemical properties of optimal electrolyte formulations. The selected formulations which were suggested from the previous model and used for conductivity determination, were added to the training set as an additional prior knowledge. Model parameters tuning and uncertainty measurement were implemented at this stage of active learning (See S4). Optimized conductivity trend for the a) 30 °C, and b) 50 °C. Trends for additional temperatures can be seen in the S3.

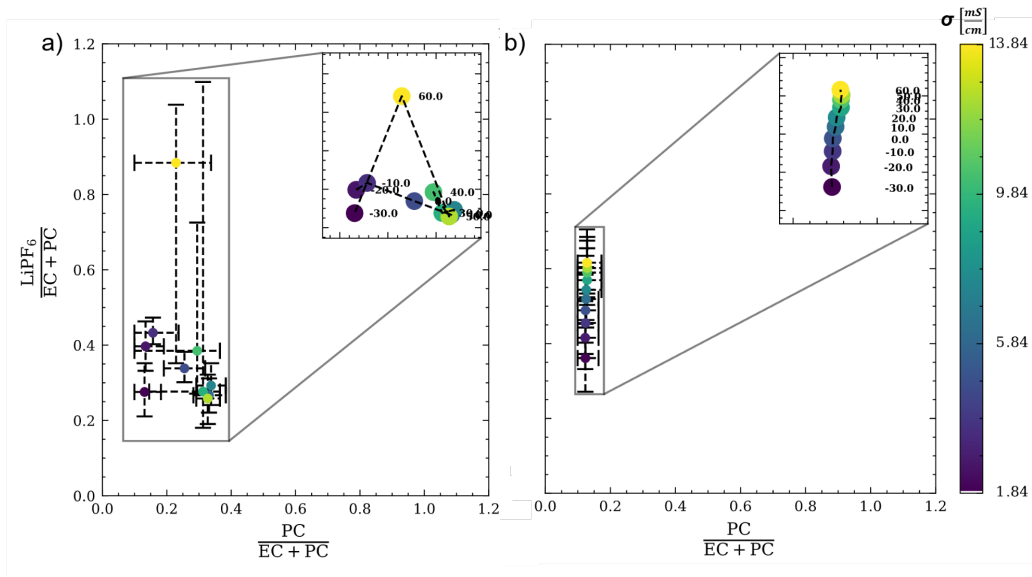


Figure 5: Trends of maximum conductivity a) before and b) after one-shot active learning and model optimization. Before introduction of the additional 24 electrolyte formulations, the trends are neither physically nor qualitatively interpretable. Each point corresponds to the mean conductivity value of the top percentile kernel. The amount required for other electrolyte solvents can be calculated as explained in the method section. The error bars represent the spread of r_{LiPF_6} and r_{PC} within the top percentile and not the uncertainty. Overall, higher r_{LiPF_6} is needed at higher temperatures to reach the optima, with a minutely higher r_{PC} from 20°C onward.

Interactions and method fidelity

Through the availability of a machine learning model that accurately and precisely predicts the trends in conductivity for all temperatures, an assessment of confounding inputs and method fidelity can be pursued. The model has two inputs: r_{PC} and r_{LiPF_6} , and through the polynomial nature an analytical derivation is facile. The post-shot regularized polynomial equation for deriving conductivity (σ) from hyperparameter tuning is:

$$\sigma = c_0 + c_1 r_{PC} + c_2 r_{LiPF_6} + c_3 r_{PC}^2 + c_4 r_{PC} r_{LiPF_6} + c_5 r_{LiPF_6}^2 + c_6 r_{PC}^3 + c_7 r_{PC}^2 r_{LiPF_6} + c_8 r_{PC} r_{LiPF_6}^2 + c_9 r_{LiPF_6}^3 \quad (\text{eq.1})$$

i.e. a polynomial of degree 3 with the individual parameters shown in Table 1. Some coefficients change drastically with temperature whilst others barely change. Upon careful comparison to eq.1, one can see that those coefficients corresponding to a conducting salt-ratio-only term, scale almost exponentially whilst all others, i.e. solvent-ratio-only and solvent-conducting salt-ratio terms scale sigmoidal with temperature (See S6.b). These interaction coefficients allow for further research into the relationship governing the solvation shell properties upon electrolyte solvent variation³⁶.

T (C°) \ c · 10 ⁻³	c ₀	c ₁	c ₂	c ₃	c ₄	c ₅	c ₆	c ₇	c ₈	c ₉
-30	1.0	-0.3	5.6	0.9	-2.3	-9.7	-0.6	1.4	0.6	4.0
-20	1.2	-0.3	8.9	0.9	-3.2	-13.6	-0.7	1.9	0.8	5.1
-10	1.4	1.0	12.1	0.1	-3.9	-17.1	-0.3	2.4	0.9	6.1
0	1.5	0.4	15.9	-0.1	-4.9	-21.2	-0.4	3.3	0.9	7.3
10	1.5	1.2	20.4	-0.9	-5.9	-26.1	-0.4	4.2	0.7	8.8
20	1.6	1.7	25.0	-1.4	-6.8	-31.0	-0.3	5.1	0.5	10.5
30	1.6	2.7	29.7	-3.2	-6.9	-35.8	0.4	5.6	0.0	12.2
40	1.6	3.0	35.1	-3.2	-7.3	-41.9	1.0	6.2	-0.6	14.6
50	1.6	3.2	41.3	-3.2	-7.6	-49.5	0.0	6.4	-0.7	17.6
60	1.6	3.0	47.4	-2.5	-6.9	-57.2	-0.7	6.6	-1.8	21.1

Table 1: Polynomial coefficients incorporating ridge regularization after one-shot active learning for T= -30 °C to 60 °C

A long lasting debate of how precise the electrolyte formulation needs to be can be answered using this model. An error propagation estimation can be done when the gradient of a function and the uncertainty of the underlying input is known. From the herein reported measurements, we know the uncertainty of the conductivity and we can easily calculate the gradient of the conductivity w.r.t. the formulation. Here, we take the median uncertainty of the conductivity measurements ($\Delta\sigma_{exp} = 3.5272 \cdot 10^{-4}$ mS/cm) and divide them by the largest gradient of conductivity w.r.t. to formulation (both uni- and bivariate) at every temperature (Figure 6) to obtain a conservative estimate of the maximally allowed formulation error (eq.2) that would be on the same order like the measurement noise. Unsurprisingly one can have larger errors in solvent-to-co-solvent ratios as in conducting salt-to-solvent ratios. Interesting however is that an error of about 10% in the solvents is acceptable for most temperatures. Dosing of the conducting salt should however be as precise as possible as at high temperatures the error should not exceed 1.5%.

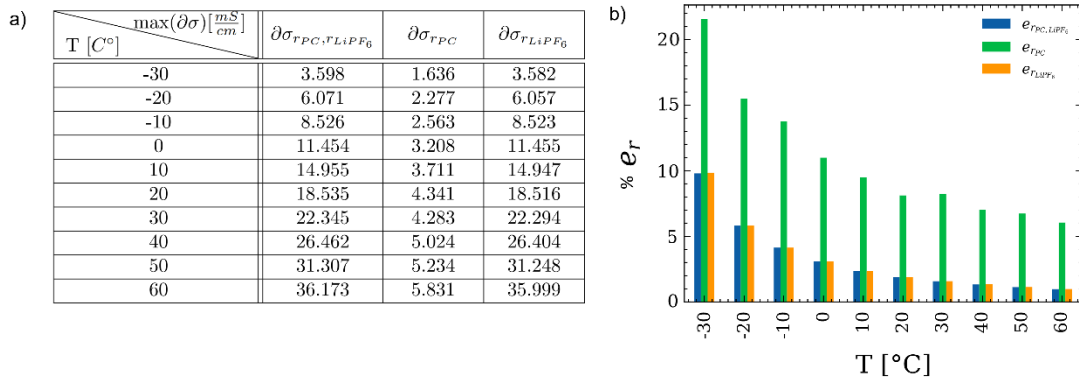


Figure 6: a) The maximum norm of predicted conductivity gradient b) the maximum formulation error calculated by eq.2 with the median $\Delta\sigma_{exp}$ of $\sim 3.5272 \cdot 10^{-4}$ mS/cm with respect to uni- and bivariate combination of r_{LiPF_6} and r_{PC} between -30 °C and 60 °C.

$$\left(\alpha \left(\frac{\partial\sigma}{\partial r_{PC}}\right)^2 + \beta \left(\frac{\partial\sigma}{\partial r_{LiPF_6}}\right)^2\right)^{0.5} \cdot e_{r_{PC}, LiPF_6} \leq \Delta\sigma_{exp} \quad \text{for} \quad \alpha, \beta \in \{(0, 1), (1, 0), (1, 1)\} \quad (\text{eq.2})$$

Conclusion

This study shows the utility of active learning to improve model accuracy and precision on complex data with few examples. The pre-shot model significantly underfit the data such that obtained trends did not follow a physically meaningful trend. After one-shot active learning, the discovered model produced smooth cross temperature optima even though it was not trained with inter temperature data. Obtained trends in the optima suggest that for low temperatures, the conducting salt concentration should be minimized whilst for higher temperatures the salt concentration should be increased. These findings are in good agreement with the DHO theory due to the activation energy being on the same order of magnitude as the temperature activation. We find that a globally optimally conducting electrolyte does not exist as those optimal at low temperatures perform poorly at high temperatures. Those electrolytes optimized for near room temperature show $\approx 20\%$ less conductivity at low and about half the conductivity at high temperatures compared to the range optimized formulations. Through the availability of an easily derivable model, we can discuss electrolyte solvent-conducting salt interactions and find mostly sigmoidal or exponential temperature trends hinting at two different mechanisms. The derivable model also allows an elucidation of maximally allowed formulation errors which lie at $\approx 10\%$ for solvents and 1.5% for conducting salts at most temperatures. Through the conservative choice of a low degree polynomial model due to scarce data availability we were able to obtain optima and interpretable insights translatable to existing physicochemical laws such as the DHO theory.

Acknowledgements

This work contributes to the research performed at CELEST (Center for Electrochemical Energy Storage Ulm-Karlsruhe) and was funded by the German Research Foundation (DFG) under Project ID 390874152 (POLiS Cluster of Excellence). This project received funding from the European Union's Horizon 2020 research and innovation programme under grant agreement No 957189.

References

- (1) Ma, S.; Jiang, M.; Tao, P.; Song, C.; Wu, J.; Wang, J.; Deng, T.; Shang, W. Temperature Effect and Thermal Impact in Lithium-Ion Batteries: A Review. *Prog. Nat. Sci. Mater. Int.* **2018**, *28* (6), 653–666. <https://doi.org/10.1016/j.pnsc.2018.11.002>.
- (2) Gupta, A.; Manthiram, A. Designing Advanced Lithium-Based Batteries for Low-Temperature Conditions. *Adv. Energy Mater.* **2020**, *10* (38), 2001972. <https://doi.org/10.1002/aenm.202001972>.
- (3) Jaguemont, J.; Boulon, L.; Dubé, Y. A Comprehensive Review of Lithium-Ion Batteries Used in Hybrid and Electric Vehicles at Cold Temperatures. *Appl. Energy* **2016**, *164*, 99–114. <https://doi.org/10.1016/j.apenergy.2015.11.034>.
- (4) Panchal, S.; Mcgrory, J.; Kong, J.; Fraser, R.; Fowler, M.; Dincer, I.; Agelin-Chaab, M. Cycling Degradation Testing and Analysis of a LiFePO₄ Battery at Actual Conditions. *Int. J. Energy Res.* **2017**, *41* (15), 2565–2575. <https://doi.org/10.1002/er.3837>.
- (5) Hubble, D.; Emory Brown, D.; Zhao, Y.; Fang, C.; Lau, J.; D. McCloskey, B.; Liu, G. Liquid Electrolyte Development for Low-Temperature Lithium-Ion Batteries. *Energy Environ. Sci.* **2022**, *15* (2), 550–578. <https://doi.org/10.1039/D1EE01789F>.
- (6) Wang, Z.; Sun, Z.; Yin, H.; Liu, X.; Wang, J.; Zhao, H.; Pang, C. H.; Wu, T.; Li, S.; Yin, Z.; Yu, X. Data-Driven Materials Innovation and Applications. *Adv. Mater.* *n/a* (n/a), 2104113. <https://doi.org/10.1002/adma.202104113>.
- (7) Rohr, B.; Stein, H. S.; Guevarra, D.; Wang, Y.; Haber, J. A.; Aykol, M.; Suram, S. K.; Gregoire, J. M. Benchmarking the Acceleration of Materials Discovery by Sequential Learning. *Chem. Sci.* **2020**, *11* (10), 2696–2706. <https://doi.org/10.1039/C9SC05999G>.

- (8) Flores, E.; Wölke, C.; Yan, P.; Winter, M.; Vegge, T.; Cekic-Laskovic, I.; Bhowmik, A. Learning the Laws of Lithium-Ion Electrolyte Transport Using Symbolic Regression. **2022**. <https://doi.org/10.26434/chemrxiv-2022-nmmd4>.
- (9) Rahmanian, F.; Flowers, J.; Guevarra, D.; Richter, M.; Fichtner, M.; Donnelly, P.; Gregoire, J. M.; Stein, H. S. Enabling Modular Autonomous Feedback-Loops in Materials Science through Hierarchical Experimental Laboratory Automation and Orchestration. *Adv. Mater. Interfaces* **2022**, 9 (8), 2101987.
- (10) Krishnamoorthy, A. N.; Wölke, C.; Diddens, D.; Maiti, M.; Mabrouk, Y.; Yan, P.; Grünebaum, M.; Winter, M.; Heuer, A.; Cekic-Laskovic, I. Data-Driven Analysis of High-Throughput Experiments on Liquid Battery Electrolyte Formulations: Unraveling the Impact of Composition on Conductivity. **2022**. <https://doi.org/10.26434/chemrxiv-2022-vbl5d>.
- (11) Cheng, X.; Khomtchouk, B.; Matloff, N.; Mohanty, P. Polynomial Regression As an Alternative to Neural Nets. *ArXiv180606850 Cs Stat* **2019**.
- (12) Ostertagová, E. Modelling Using Polynomial Regression. *Procedia Eng.* **2012**, 48, 500–506. <https://doi.org/10.1016/j.proeng.2012.09.545>.
- (13) Johnston, R.; Jones, K.; Manley, D. Confounding and Collinearity in Regression Analysis: A Cautionary Tale and an Alternative Procedure, Illustrated by Studies of British Voting Behaviour. *Qual. Quant.* **2018**, 52 (4), 1957–1976. <https://doi.org/10.1007/s11135-017-0584-6>.
- (14) Marcoulides, K. M.; Raykov, T. Evaluation of Variance Inflation Factors in Regression Models Using Latent Variable Modeling Methods. *Educ. Psychol. Meas.* **2019**, 79 (5), 874–882. <https://doi.org/10.1177/0013164418817803>.
- (15) Wooldridge, J. M. *Introductory Econometrics: A Modern Approach*; Cengage Learning, 2015.
- (16) Vittinghoff, E.; Glidden, D. V.; Shiboski, S. C.; McCulloch, C. E. Linear Regression. In *Regression Methods in Biostatistics: Linear, Logistic, Survival, and Repeated Measures Models*; Vittinghoff, E., Glidden, D. V., Shiboski, S. C., McCulloch, C. E., Eds.; Springer US: Boston, MA, 2012; pp 69–138. https://doi.org/10.1007/978-1-4614-1353-0_4.
- (17) James, G.; Witten, D.; Hastie, T.; Tibshirani, R. *An Introduction to Statistical Learning: With Applications in R*; Springer Texts in Statistics; Springer US: New York, NY, 2021. <https://doi.org/10.1007/978-1-0716-1418-1>.
- (18) Menard, S. *Applied Logistic Regression Analysis*; SAGE, 2002.
- (19) McDonald, G. C. Ridge Regression. *WIREs Comput. Stat.* **2009**, 1 (1), 93–100. <https://doi.org/10.1002/wics.14>.
- (20) Buitinck, L.; Louppe, G.; Blondel, M.; Pedregosa, F.; Mueller, A.; Grisel, O.; Niculae, V.; Prettenhofer, P.; Gramfort, A.; Grobler, J.; Layton, R.; Vanderplas, J.; Joly, A.; Holt, B.; Varoquaux, G. API Design for Machine Learning Software: Experiences from the Scikit-Learn Project. *ArXiv13090238 Cs* **2013**.
- (21) Hackeling, G. *Mastering Machine Learning with Scikit-Learn*; Packt Publishing Ltd, 2017.
- (22) Kramer, O. Scikit-Learn. In *Machine Learning for Evolution Strategies*; Kramer, O., Ed.; Springer International Publishing: Cham, 2016; pp 45–53. https://doi.org/10.1007/978-3-319-33383-0_5.
- (23) Wu, J.; Chen, X.-Y.; Zhang, H.; Xiong, L.-D.; Lei, H.; Deng, S.-H. Hyperparameter Optimization for Machine Learning Models Based on Bayesian Optimization. *J. Electron. Sci. Technol.* **2019**, 17 (1), 26–40. <https://doi.org/10.11989/JEST.1674-862X.80904120>.
- (24) *MAPIE - Model Agnostic Prediction Interval Estimator — MAPIE 0.3.2 documentation*. <https://mapie.readthedocs.io/en/latest/index.html> (accessed 2022-04-13).
- (25) Barber, R. F.; Candès, E. J.; Ramdas, A.; Tibshirani, R. J. Predictive Inference with the Jackknife+. *Ann. Stat.* **2021**, 49 (1), 486–507. <https://doi.org/10.1214/20-AOS1965>.
- (26) Hüllermeier, E.; Waegeman, W. Aleatoric and Epistemic Uncertainty in Machine Learning: An Introduction to Concepts and Methods. *ArXiv191009457 Cs Stat* **2020**.
- (27) Hall, D. S.; Self, J.; Dahn, J. R. Dielectric Constants for Quantum Chemistry and Li-Ion Batteries: Solvent Blends of Ethylene Carbonate and Ethyl Methyl Carbonate. *J. Phys. Chem. C* **2015**, 119 (39), 22322–22330. <https://doi.org/10.1021/acs.jpcc.5b06022>.
- (28) Ding, M. S.; Jow, T. R. Physicochemical Properties of Non-Aqueous Solvents and Electrolytes for Lithium Battery Applications. *ECS Trans.* **2009**, 16 (35), 183. <https://doi.org/10.1149/1.3123139>.
- (29) Landesfeind, J.; Gasteiger, H. A. Temperature and Concentration Dependence of the Ionic Transport Properties of Lithium-Ion Battery Electrolytes. *J. Electrochem. Soc.* **2019**, 166 (14), A3079. <https://doi.org/10.1149/2.0571912jes>.
- (30) Ding, M. S.; Jow, T. R. Conductivity and Viscosity of PC-DEC and PC-EC Solutions of LiPF₆. *J. Electrochem. Soc.* **2003**, 150 (5), A620. <https://doi.org/10.1149/1.1566019>.

- (31) Hayamizu, K. Temperature Dependence of Self-Diffusion Coefficients of Ions and Solvents in Ethylene Carbonate, Propylene Carbonate, and Diethyl Carbonate Single Solutions and Ethylene Carbonate + Diethyl Carbonate Binary Solutions of LiPF₆ Studied by NMR. *J. Chem. Eng. Data* **2012**, 57 (7), 2012–2017. <https://doi.org/10.1021/je3003089>.
- (32) Hay, K. A.; Hicks, F. G.; Holmes, D. R. The Transport Properties and Defect Structure of the Oxide (Fe, Cr)₂O₃ formed on Fe-Cr alloys. *Mater. Corros. Korros.* **1970**, 21 (11), 917–924. <https://doi.org/10.1002/maco.19700211107>.
- (33) Ding, M. S.; Li, Q.; Li, X.; Xu, W.; Xu, K. Effects of Solvent Composition on Liquid Range, Glass Transition, and Conductivity of Electrolytes of a (Li, Cs)PF₆ Salt in EC-PC-EMC Solvents. *J. Phys. Chem. C* **2017**, 121 (21), 11178–11183. <https://doi.org/10.1021/acs.jpcc.7b03306>.
- (34) Ding, M. S.; Jow, T. R. How Conductivities and Viscosities of PC-DEC and PC-EC Solutions of LiBF₄, LiPF₆, LiBOB, Et₄NBF₄, and Et₄NPF₆ Differ and Why. *J. Electrochem. Soc.* **2004**, 151 (12), A2007. <https://doi.org/10.1149/1.1809575>.
- (35) Naejus, R.; Lemordant, D.; Coudert, R.; Willmann, P. Excess Thermodynamic Properties of Binary Mixtures Containing Linear or Cyclic Carbonates as Solvents at the Temperatures 298.15 K and 315.15 K. *J. Chem. Thermodyn.* **1997**, 29 (12), 1503–1515. <https://doi.org/10.1006/jcht.1997.0260>.
- (36) Siegel, D. J.; Nazar, L.; Chiang, Y.-M.; Fang, C.; Balsara, N. P. Establishing a Unified Framework for Ion Solvation and Transport in Liquid and Solid Electrolytes. *Trends Chem.* **2021**, 3 (10), 807–818. <https://doi.org/10.1016/j.trechm.2021.06.004>.